에너지공학, 제17권 제2호(2008)
Journal of Energy Engineering, Vol. 17, No. 2, pp. 47~53 (2008)

Performance Analysis of Carbon Canister for Reducing Evaporative Emissions in a Gasoline Automotive Engine

Yon Jong Chung*, Gyu Sang Cho*, Paul A. Erickson and Sung Bin Han***,†**

**Department of Automotive Engineering, Daegu Mirae College,*
270 Pyungsan-dong, Kyungsan-si, Kyungsangbuk-do 712-716, Korea
***Mechanical and Aeronautical Engineering Department, University of California Davis, Davis, CA 95616, USA*
****Department of Mechanical & Automotive Engineering, Induk Institute of Technology,*
San 76 Wolgye-dong, Nowon-gu, Seoul 139-749, Korea

(Received 5 November 2007, Revised 4 April 2008, Accepted 14 April 2008)

Abstract — The objective of this paper is to clarify the flow characteristic, velocity distribution, pressure loss, and other such fundamental data for the canister during loading and purging. The amount of gas that is loaded increases as the loading rate is decreased and the time increased, and the purging improves as the purge rate is increased. The hydrocarbons that are purged initially have a high concentration, and a large amount is purged. During loading and purging, the temperature initially increases and decreases drastically due to heat generation and heat loss.

Key words: Evaporative emissions, Fuel vaporization, Canister, Loading, Purging, Purge control solenoid valve (PCSV)

1. Introduction

Canister refers to a device which stores the evaporation gas that has evaporated from the fuel tank. Instead of expelling it to the atmosphere, the canister supplies the stored gas to the combustion chamber upon ignition. The use of a canister allows the evaporation gas to be reused and reduces environmental pollution attributed to it. Conventional exhaust gas is produced during the operation of the vehicle, but evaporation gas is a source of air pollution that does not depend on the vehicle's operation[1][2].

Automotive exhaust emission regulations are becoming progressively stricter due to increasing awareness of the hazardous effects of exhaust emissions. Improving fuel economy and reducing emissions are two major tasks challenging automotive engineers today[3].

Evaporative hydrocarbon emissions from gasoline-powered vehicles continue to be a major concern in areas where the national ambient air quality standard for ozone is violated. Evaporative emissions are generally grouped into the following basic categories: running losses, hot soak emissions, and diurnal emissions. The latter category is usually divided into two subcategories: resting losses and pressure-driven diurnal emissions[4].

A vehicle's evaporative emission control system is continuously working, even when the vehicle is not running, due to generation of vapors from the fuel tank during ambient temperature variations. Diurnal temperature cycles cause the fuel tank to breathe the fuel vapor in and out, and thus the activated carbon canister is constantly loading and purging the hydrocarbon vapors[5].

For the loading and purging of the canister evaporative gas when it is installed on a vehicle, the amount of purge air, loading rate, and other such characteristics must be clarified. In addition, the effects on the engine during loading and purging must be understood so that the canister can be designed to take full advantage of the loading and purging characteristics. Recently, a fuel vapor system model has been developed to simulate vehicle evaporative emission control system behavior[6][7].

†To whom correspondence should be addressed.
Department of Mechanical & Automotive Engineering, Induk Institute of Technology, San 76 Wolgye-dong, Nowon-gu, Seoul 139-749, Korea
Tel: 02-950-7545
E-mail: sungbinhan@induk.ac.kr

The fuel system components incorporated into the model include the fuel tank and pump, filler cap, liquid supply and return lines, fuel rail, vent valves, vent line, carbon canister and purge line. The system is modeled as a vented system of liquid fuel and vapor in equilibrium, subject to a thermal environment characterized by under-hood and under-body temperatures and heat transfer parameters assumed known or determined by calibration with experimental liquid temperature data. Numerical calculation has allowed canister purge algorithm with a virtual sensor and several studies have reported a carbon canister model[8]-[10].

The objective of this paper is to clarify the flow characteristic, velocity distribution, pressure loss, and other such fundamental data for the canister during loading and purging. The experimental results show the effectiveness of this system for future exhaust emissions and enhanced evaporative emissions.

2. Experimental Setup and Procedure

Figure 1 shows the cross-sectional view of the canister. There are three openings to the canister: Inlet for the evaporation gas to enter from the fuel tank, exit leading to the intake port of the engine, and a purge port for the clean, external air. On the top and bottom sections of the cylindrical canister are 3 mm thick filters and a grid, and there is an air gap between the filter and the port. The interior of the canister is filled with activated carbons.

Figure 2 shows the schematic diagram of the canister and the measurement locations. To clarify the temperature distribution characteristics within the canister at loading and purging, a total of 30 T type thermocouples were installed. Temperature measurements were taken at 10 second intervals using Multiscan/1200

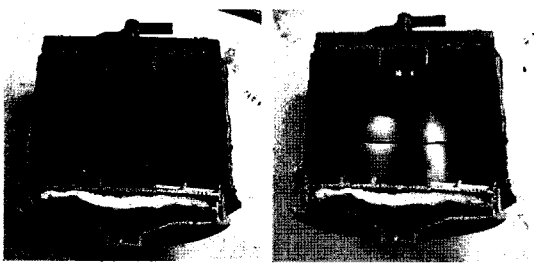

Fig. 1. Cross-sectional view of the canister.

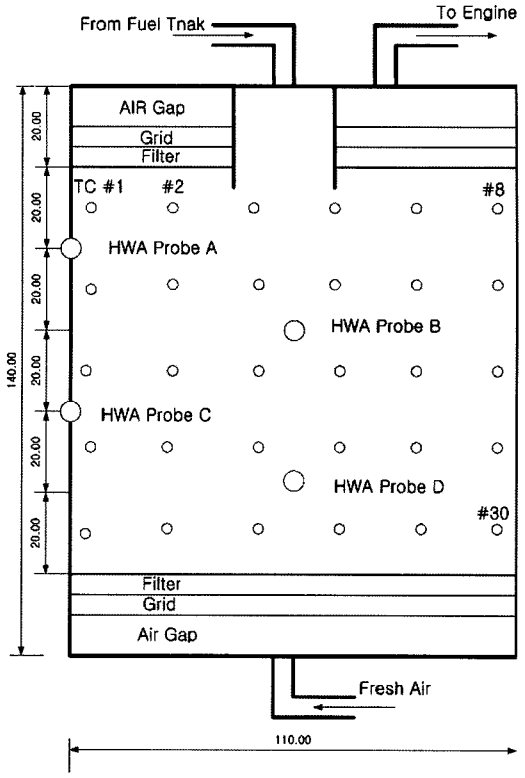

Fig. 2. Schematic diagram of the canister and the measurement locations.

from IOtech, and data were acquired using Chartview. Pressure loss was measured with a pressure gauge located at each port. In order to understand the flow characteristics of the evaporation gas within the canister, a flow characteristic testing apparatus was constructed. To clarify the canister characteristics and HC emissions were measured when the hydrocarbon flowed into the canister. For the loading and purging of the canister fuel vapor when it is installed on a vehicle, it must be clarified. In addition, the effects on the engine during loading and purging must be understood so that the canister can be designed to take full advantage of the loading and purging characteristics. To control the hydrocarbon concentration that flows in afterwards, the amount of nitrogen was the adjusted proportion. The experiments were performed in three steps at nitrogen versus hydrocarbon per volume proportions 100/0, 75/25, and 50/50.

During loading, the vacuum pump was connected to the fresh air part of the canister with the purge

valve closed, and flow was controlled using the inlet valve and measured using a laminar flow meter. During purging, the location of the vacuum pump was switched, and the air was purged at the same flow rate. Loading was performed in four steps at 0.3 *l*, 0.6 *l*, 0.9 *l*, and 3 *l* per minute while purging was done in four steps at 6.0 *l*, 7.8 *l*, 15.0 *l*, and 21.0 *l* per minute.

A vacuum pump was used to inject and extract air to simulate loading and purge conditions. The flow rate of this air was measured using a laminar flow meter, and the velocity distribution within the canister was measured using a constant temperature anemometer. Temperature was measured using a platinum hot wire probe with a diameter of 5 μm, and the measurement locations were 20 mm and 60 mm from the top and 40 mm and 80 mm in the vertical direction, for a total of four locations at 10 mm depth increments measuring the velocity in the radial direction.

3. Results and Discussion

Figure 3 shows the hydrocarbon volume at different loading rates. In this figure, the inflow of gas into the canister is increasing proportionally to time. Since the amount of loading gradually increases as loading rate is decreased, the loading rate should be minimized to allow absorption. When the loading rate is increased, the temperature of the canister increases significantly due to heat generated during loading. The temperature reaches 80°C at times, and has an adverse effect on absorption. As the volume of hydrocarbons increase, the weight of the gas also

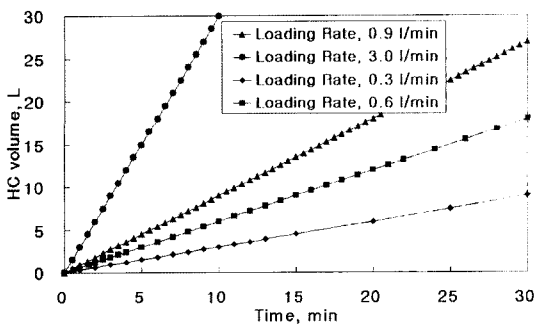

Fig. 3. Hydrocarbon volume vs. time at different loading rates.

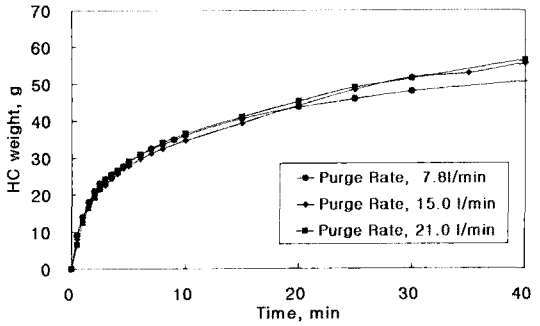

Fig. 4. Relationship between time and hydrocarbon weight at different purge rates.

increases gradually. When the loading rate is 3.0 *l*/min, 75 kg is absorbed, and when the loading rate is 0.3 *l*/min, up to 150 kg is absorbed.

Figure 4 shows the time dependence of the HC weight at different purge rates. A large amount of hydrocarbon is purged initially and slowly increases as time goes on. The amount of hydrocarbons purged increases with the purge rate, but the change is very small. The volume of hydrocarbons that is desorbed is dependent on time. Generally, the total amount of air that passes through the activated carbon bed is the product of the purge rate and purge time, and this is defined as the purge bed volume.

Figure 5 shows the weight of the hydrocarbon as a function of the purge bed volume at different purge rates. The amount of hydrocarbons that is desorbed increases as the purge bed volume increases. When the purge bed volume is small, the amount of hydrocarbons that is desorbed decreases abruptly, and after a certain bed volume, the amount desorbed gradually

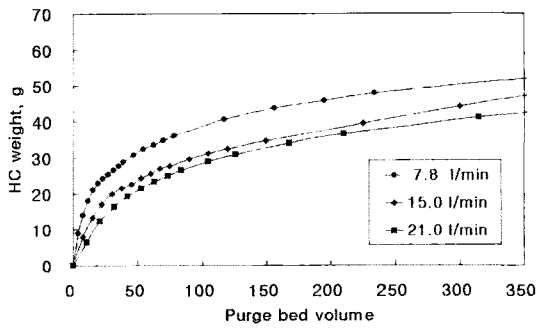

Fig. 5. Relationship between purge bed volume and hydrocarbon weight for purge rates.

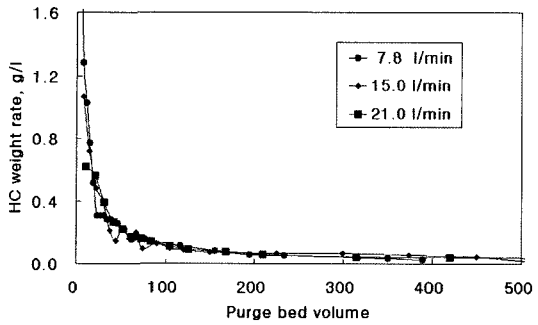

Fig. 6. Relationship between purge bed volume and hydrocarbon weight rate for purge rates.

increases. Namely, a large amount exits upon desorption early during purging, and since the amount purged continues to decrease, we know that a large amount of hydrocarbons will be desorbed in an actual engine during the early stage of a PCSV's opening.

Figure 6 shows the weight of the hydrocarbons in the purged vapor as a function of the purge bed volume. The weight of the hydrocarbons is large when the purge bed volume is small, but it decreases rapidly as the purge bed volume increases. This shows that, in the early stages of an PCSV's operation, highly concentrated gas flows into the engine, whereas a dilute gas flows in afterwards. Since it is more likely for the engine to be in a bad condition in the latter stage than in the early stage, canister and the engine must be taken into consideration in the designing of the PCSV operation time setup mode.

Figures 7 and 8 show the temperature differences during absorption and desorption as a function of time at varying canister locations. It can be seen that heat generated during loading initially causes a signif-

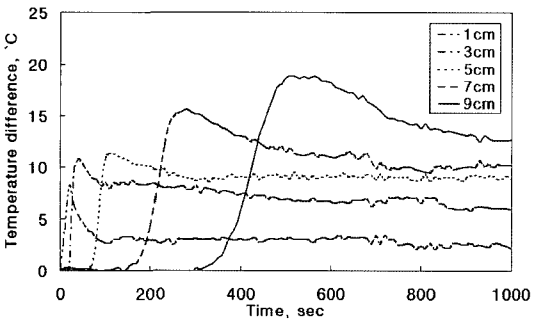

Fig. 7. Temperature difference vs. time during loading.

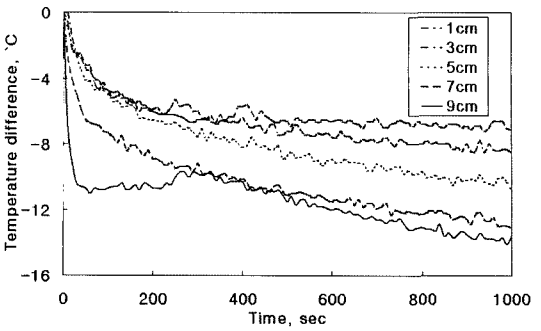

Fig. 8. Temperature difference vs. time during purging.

icant temperature increase but later decreases gradually. Upon desorption, the reverse process of heat absorption is shown. Distribution during absorption and desorption shows that the hydrocarbons are absorbed desorbed gradually from the port entrance towards the center and becomes symmetric as time passes, showing a distribution with no dead zone. When the evaporation gas is supplied to the canister, the activated carbon within the canister initiates the loading process, and heat is generated from the exothermic process. Traditionally, in order to observe the loading characteristics, the concentration of the evaporation gas that is absorbed by the activated carbon should be measured, but due to technical and financial restrictions, the temperature rise during the loading process is measured instead. Although this method may be indirect, loading level and loading distribution of the evaporation gas due to the activated carbon should be

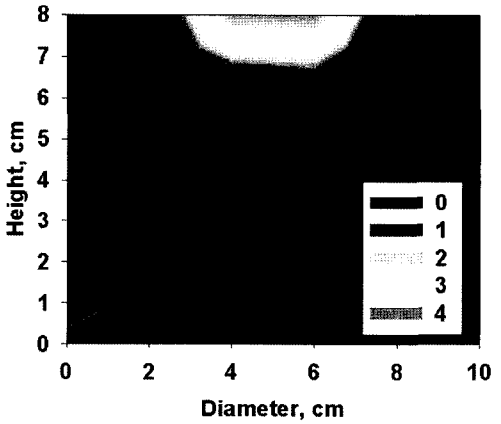

Fig. 9. Temperature distribution for varying bed locations 10 seconds after loading.

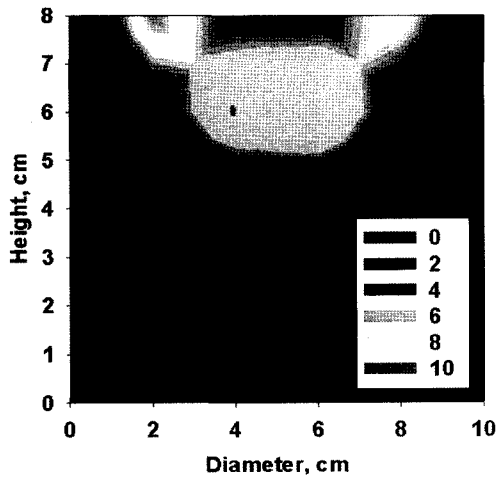

Fig. 10. Temperature distribution for varying bed locations 60 seconds after loading.

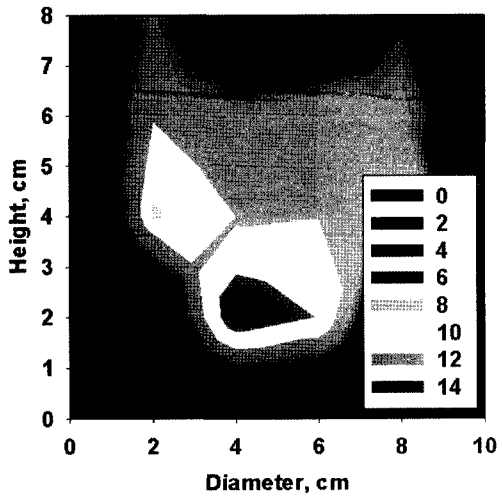

Fig. 11. Temperature distribution for varying bed locations 240 seconds after loading.

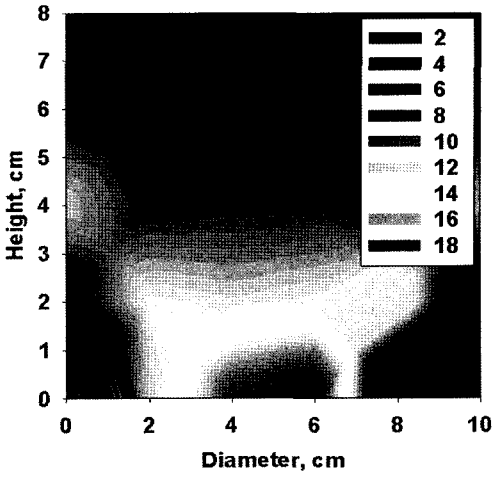

Fig. 12. Temperature distribution for varying bed locations 480 seconds after loading.

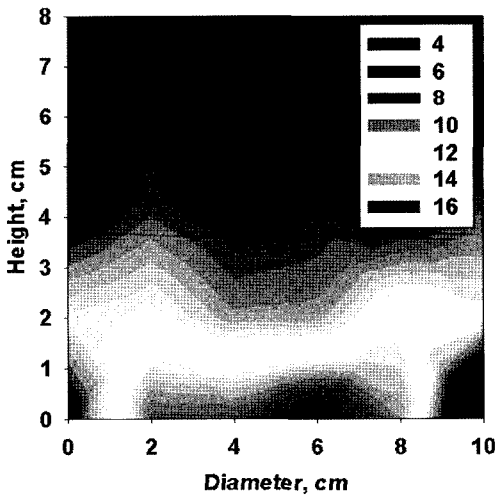

Fig. 13. Temperature distribution for varying bed locations 720 seconds after loading.

able to be determined. Therefore, a thermocouple was inserted into the canister, and temperature distribution as a function of time is shown.

In Figs. 9~13, the region shown in red seems to be the result of a temperature rise caused by the loading/ exothermic process. The evaporation gas is supplied to the top of the canister and is shown in red due to the exothermic process that starts from this location. It is seen that the evaporation gas enters from the bottom of the canister and results in an exothermic process. The temperature rises and then falls in the rear section due to the cooling effect of the continuously supplied evaporation gas. This shows that the evaporation gas has already reached its saturation point, and the loading effect is no longer taking place in this section. In addition, the shape of the canister takes into consideration internal flow and is likely responsible for the elimination of the dead zone.

Figures 14~18 show the process of purging the evaporation gas by supplying fresh air to the bottom

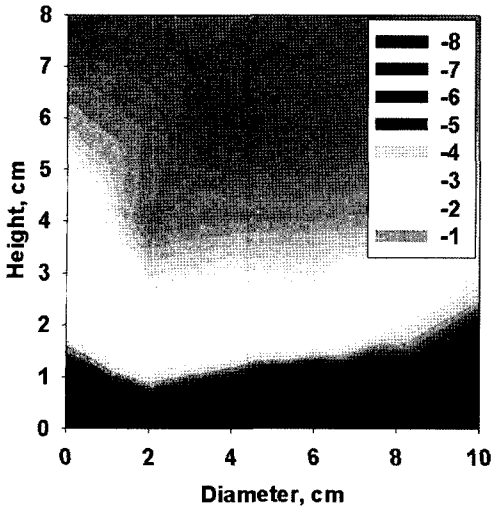

Fig. 14. Temperature distribution for varying bed locations 10 seconds after purging.

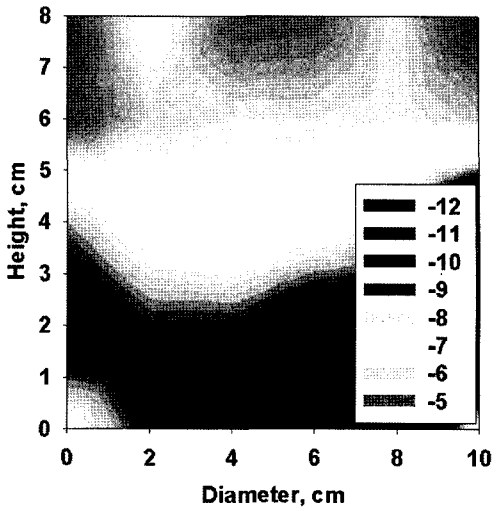

Fig. 16. Temperature distribution for varying bed locations 240 seconds after purging.

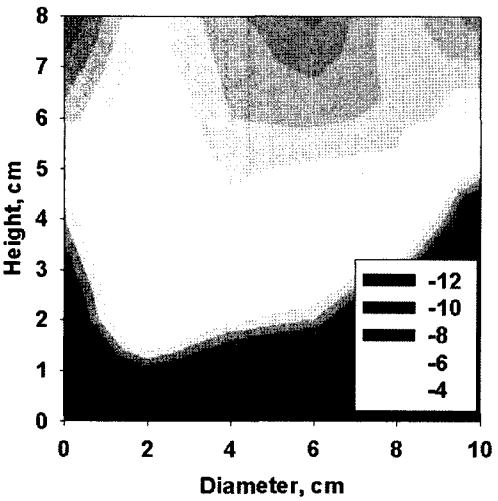

Fig. 15. Temperature distribution for varying bed locations 60 seconds after purging.

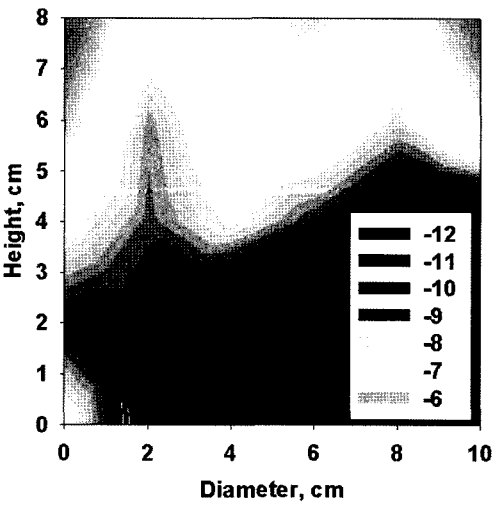

Fig. 17. Temperature distribution for varying bed locations 480 seconds after purging.

of the saturated canister and then supplying the returned evaporation gas to the engine's combustion chamber. As the figure shows, temperatures inside the canister decrease during the purging process due to the endothermic process. In other words, the purging process occurs in the region of decreasing temperature. Also, as time passes, fresh air is supplied to the bottom part of the canister and the loaded evaporation gas is purged; the temperature gradually decreases due to the endothermic process. However, this process does not show a region of increased temperature that occurs after saturation during the loading process. This shows that the purging process is not completed as quickly as the loading process. Purging must be completed in a short period of time in order for the loading process to take place again at the start-stop condition, but the extended purging process is expected to disturb the loading process. The developmental

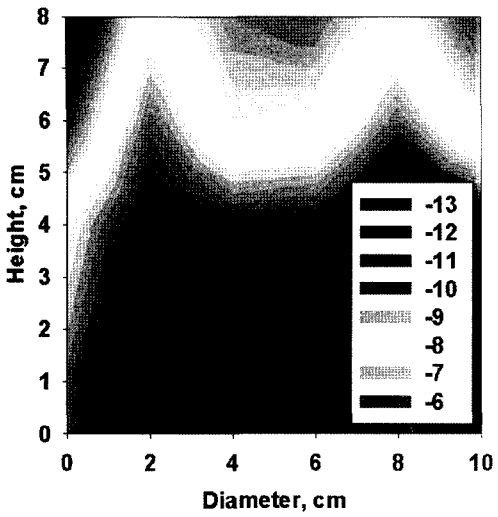

Fig. 18. Temperature distribution for varying bed locations 720 seconds after purging.

focus of a high performance canister should be to build the canister in such a way that the purging process is completed in a short period of time.

4. Conclusions

The amount of gas that is loaded increases as the loading rate is decreased and the time increased, and the purging improves as the purge rate is increased. The hydrocarbons that are purged initially have a high concentration, and a large amount is purged. During loading and purging, the temperature initially increases and decreases drastically due to heat generation and heat loss. Afterwards, the temperature changes gradually, and the even temperature distribution throughout the canister indicates that the dead zone is almost non-existent.

Acknowledgments

This research was partially supported by the 2007 sabbatical program at Daegu Mirae College, Korea.

References

1. Johnson, P.J.; Jamrog, J.R.; Lavoie, G.A. Activated carbon canister performance during diurnal cycles : An experimental and modeling evaluation, SAE paper 971651, 1997.
2. Haskew, H.M.; Liberty, T.F. Diurnal emissions from in-use vehicle, SAE paper 1999-01-1463, 1999.
3. Yang, J.; Culp, T.; Kenney, T. Development of a gasoline engine system using HCCI technology - the concept and the test results. SAE paper 2002-01-2832, 2002.
4. Lyons, J.M.; Lee, J.M.; Heirigs, P.L.; McClement, D.; Welstand, S. Evaporative emissions from late-model in-use vehicles, SAE paper 2000-01-2958, 2000.
5. Haskew, H.M.; Eng, K.D.; Liberty, T.F. Running loss emission from in-use vehicle, SAE paper 1999-01-1464, 1999.
6. Lavoie, G.A.; Imai, Y.A.; Johnson, P.J. A fuel vapor model (FVSMOD) for evaporative emissions system design and analysis, SAE paper 982644, 1998.
7. Yoo, I.K.; Upadhyay, D.; Rizzoni, G.A. Control-oriented carbon canister model, SAE paper 1999-01-1103, 1999.
8. Grieve, M.J.; Himes, E.G. Advanced canister purge algorithm with a virtual HC sensor, SAE paper 2000-01-0557, 2000.
9. Lavoie, G.A.; Johnson, P.J.; Hood, J.F. Carbon canister modeling for evaporative emissions: Adsorption and thermal effects, SAE paper 981210, 1998.
10. Matsushima, H.; Iwamoto, A.; Ogawa, M.; Satoh, T.; Ozaki, K. Development of a gasoline-fueled vehicle with zero evaporative emissions, SAE paper 2001-01-2926, 2001.